Therapeutic effects of silver nanoparticles on *Escherichia coli*-induced endometritis in rats

Amal M. Aboelmaaty[a], Mohamed A. Sayed[a], Mahmoud A. Elgabry[a], Mohamed S. Kotp[a], Ghadha I. Fouad[b], Marwa E. El-Shamarka[c], Ehab A. Fouad[d], Ashraf H. Soror[a], Shimaa T. Omara[d]

[a]Department of Animal Reproduction and Artificial Insemination, Veterinary Research Institute, Dokki, Giza, Egypt, [b]Department of Therapeutic Chemistry, Pharmaceutical and Drug Industries Research Institute, Dokki, Giza, Egypt, [c]Department of Narcotics, Ergonomic Aids and Poisons, Medical Research Institute, Dokki, Giza, Egypt, [d]Department of Microbiology and Immunology, Veterinary Research Institute, National Research Centre, Dokki, Giza, Egypt

Correspondence to Amal M. Aboelmaaty, PhD, Department of Animal Reproduction and AI, Veterinary Research Institute, National Research Centre, 33 ElBuhouth Street, Dokki, Giza 12622, Egypt Tel: 01221278132; e-mail: amalaboelmaaty1@yahoo.com, am.aly@nrc.sci.eg

Received: 26 June 2022
Revised: 23 July 2022
Accepted: 24 July 2022
Published: 8 November 2022

Egyptian Pharmaceutical Journal 2022, 21:456–471

Background
Silver nanoparticles (AgO-NPs) have shown antimicrobial effects against a broad spectrum of microorganisms.
Objectives
To assess the antimicrobial effects of AgO-NPs prepared using an eco-friendly green method against multidrug-resistant *Escherichia coli in vivo* after inducing endometritis in rats.
Materials and methods
In female mice, LD_{50} of AgO-NPs was determined, followed by a chronic toxicity in female rats by oral administration of 0, 20, 30, and 40 mg of AgO-NPs daily for 4 weeks. The induced endometritis model in female rats was performed by inoculating two doses of *E. coli* (100 µl of 10×10^5 CFU) intravaginally. Seven days later, vaginal swabs were stained with Wright stain to confirm the development of endometritis and used to re-isolate the inoculated microorganism. Two doses of 100 µl containing 10 mg AgO-NPs were inoculated intravaginally. Estradiol, progesterone, liver and kidney functions, oxidants and antioxidants, and zinc were measured in collected blood samples of chronic toxicity and induced endometritis model.
Results and conclusion
LD_{50} of AgO-NPs was 800 mg/kg body weight (BW). The use of 40 (1 : 20 LD_{50}), 30 (1 : 26.67 LD_{50}), and 20 (1 : 40 LD_{50}) mg/kg BW during the chronic toxicity experiment was safe as indicated by blood biochemical analyses. The chronic toxicity experiment resulted in normal liver and kidney functions, oxidant–antioxidant status, acute-phase proteins, and ovarian hormones. The green method-synthesized AgO-NPs showed efficacy against *E. coli*-induced endometritis, and rats responded to the treatment as indicated by the uterine cytology and the clinical analysis with mild adverse effects on both liver and kidney. In conclusion, AgO-NPs showed treatment of experimental uterine infections induced by *E. coli* in rats and were safe for longer administration in concentrations lower than 50 mg/kg BW.

Keywords:
acute-phase response, induced endometritis, nanosilver chronic toxicity, ovarian hormones, oxidants–antioxidants, rats

Egypt Pharmaceut J 21:456–471

1687-4315

Introduction

In equine, endometritis is considered one of the major causes of infertility [1]. Endometritis is usually caused by mixed bacterial infections, including *Escherichia coli* [2]. Pro-inflammatory cytokines are always associated with bacterial endometritis [3]. Directly after natural or experimental infections, the animal body responds to the *E. coli* lipopolysaccharide (LPS) by secreting the toll-like receptor-4 from the endometrial epithelial cells to activate mitogen-activated protein kinase and downstream nuclear factor κB pathways, stimulating the release of cytokines [2]. These inflammatory mediators often disturb the normal physiology of the uterus and produce injury to the uterus accompanied with histopathological lesions [4]. Both inflammatory mediators as well as *E. coli* LPS showed disturbed hypothalamic–pituitary–ovarian axis, suppressed ovulations, delayed or blocked the luteinizing hormone surge, reduced estradiol rise, decreased conception, and induced embryonic loss [5]. On the contrary, inhibition and/or suppression of these pro-inflammatory cytokines attenuated bacterial endometritis [6]. Duchesne *et al.* [7] identified that *E. coli* was one of the most frequently isolated pathogens from equine endometrium, reaching

20.0%. de Lagarde *et al.* [8] reported that 44% of infected horses shed multidrug-resistant *E. coli*. Resistance was observed to ampicillin, streptomycin, and amoxicillin/clavulanic acid.

Silver nanoparticles (AgO-NPs) prepared by the physical approach produced pure NPs compared with the chemical approach [9]. The use of eco-friendly green method using plant extract has been proved to be a safe, rapid, and effective method [10]. *Thymus vulgaris* (thyme) is one of the oldest Egyptian antimicrobial plants. It inhibited the growth of *Pseudomonas* with the individual extract and when it was used in lower concentrations with ineffective antibiotics [11]. Using HPLC, thyme contained 16 compounds of essential oils and the main phenolic and flavonoid compounds of ethanolic extracts identified were salicylic, ellagic, hesperidin, and rosmarinic [12]. The green synthesis of AgO-NPs with *Phyllanthus amarus* and *Panax ginseng* leaves [13,14], *Persea americana* seeds [15], *Ziziphus jujuba* leaves [16], *Camellia sinensis* leaves [17], and *Elettaria cardamomum* seeds [18] showed antimicrobial effects against a wide range of bacteria including *E. coli* [19].

T. vulgaris (thyme) was used to synthesize zinc NPs and showed antibacterial effects against *E. coli in vitro* [20] and its LPS *in vivo* [21]. Our aims were to synthesize AgO-NPs using thyme and to determine its LD_{50}, chronic toxicity, and its therapeutic effect against *E. coli*-induced endometritis in rats to determine the clinical biochemical responses and the reproductive hormones.

Materials and methods

Before performing any laboratory animal experiments, the approval of the Animal Care and Use Committee of the National Research Center and Medical Research Ethics Committee number (NRC-19-143) was obtained. All animal experiments were carried out in accordance with the U.K. Animals (Scientific Procedures) Act, 1986, and associated guidelines, the European Communities Council Directive of November 24, 1986 (86/609/EEC), or the National Institutes of Health guide for the care and use of laboratory animals (NIH Publications No. 8023, revised 1978).

Collection of samples from uteri of mares

An equine cytobrush (Minitube, Germany) was introduced into the uterus and then samples were spread on glass slides and stained with Wright's stain for counting the number of neutrophils and confirming endometritis. Then, both the cytobrush and double guarded swab (Minitube) were covered by 5-ml sterile phosphate buffer in sterilized 15.0-ml Falcon tubes to be cultured within 24 h [22]. Uterine wash was performed using equine Y-junction with Foley catheter (Minitube) to use 250–500 ml (Saline or Ringer's solutions), and the reflux was sent to the laboratory for bacterial culture.

The bacterial culture

Samples were inoculated into sterile tubes containing brain–heart infusion broth (BHI, Oxoid Limited, Wade Road, Basingstoke Hampshire, RG24 8PW, United Kingdom). The broth was then transferred in an insulated ice box to the Department of the Microbiology and Immunology, Veterinary Institute, National Research Center (NRC), Cairo, Egypt, where they were analyzed immediately for the presence of any bacterial pathogen. All samples were incubated for 24 h at 37°C. A loopful from each broth was then streaked into the following agar medium: brain–heart infusion agar (BHI, Oxoid), MacConkey's agar (Oxoid), *Pseudomonas* agar medium (Oxoid) supplemented with *Pseudomonas* CFC supplement (SR0103), blood agar (Oxoid) supplemented with 5% sheep red blood cells, *Salmonella Shigella* agar (Oxoid), mannitol salt agar (MSA, Oxoid), and Baird-Parker agar (BP, Oxoid) supplemented with Egg Yolk-Tellurite Emulsion (SR0054, Oxoid). All plates were then incubated aerobically at 37°C for 24–48 h. Identification of the recovered isolates was done according to Koneman's Color Atlas and Textbook of Diagnostic Microbiology [23] and also using API kit (bioMérieux Deutschland GmbH, Weberstrasse 8 D-72622 Nürtingen, Darmstadt, Germany) according to the manufacturer's instructions. The confirmed isolates were preserved with 15% glycerol at -80°C.

Antimicrobial susceptibility of the isolated microorganisms

Antimicrobial sensitivity was achieved by the Kirby-Bauer disk diffusion method based on the National Committee for Clinical Laboratory Standards [23] using the Mueller-Hinton agar (Oxoid) and the following antimicrobial impregnated disks (Oxoid) for *Pseudomonas aeruginosa*: ceftazidime (30 μg), gentamicin CN (10 μg), amikacin (30 μg), aztreonam (30 μg), cefepime (30 μg), ciprofloxacin (5 μg), imipenem (10 μg), piperacillin tazobactam (100/10 μg). However, for the other isolated microorganisms, the following antimicrobial impregnated disks (Oxoid) were used: cefazolin

(30 μg), gentamicin CN (10 μg), amikacin (30 μg), amoxicillin/clavulanic acid (30 μg), cefepime (30 μg), cefoxitin (30 μg), cefotaxime (30 μg), ciprofloxacin (5 μg), imipenem (10 μg), ceftazidime (30 μg), chloramphenicol (30 μg), and tetracycline (30 μg). All plates were then incubated at 37°C for 24 h, and the zones of inhibition were measured and interpreted according to National Committee for Clinical Laboratory Standards guidelines [24].

Preparation of silver nanoparticles

AgO-NPs were prepared using the aqueous plant extract of thymus (*T. vulgaris*) purchased from commercial herbal stores. Overall, 20.0 g of the dried plant was added to 200 ml of bidistilled water and kept at 37°C and then rotated at 200 rpm in a shaker incubator (Thermo Fisher Scientific. 168 Third Avenue. Waltham, MA USA 02451) for 48 h. To each 1 g of extra pure silver nitrate (molecular weight 169.87, SDFCL, s d fine-chemical limited, Mumbai, Maharashtra, India.), 10 ml of the filtrated plant extract was added and stirred using a glass rod or magnetic heat stirrer until the complete conversion of the soluble white salt into diffuse insoluble suspended silver oxide crystals of brown to black color that can be seen by the naked eye [13–17]. Particle size distribution was determined using a transmission electron microscope (TEM; JEOL HR-TEM, JEM-2100, Japan). The aqueous solution of AgO-NPs was left in the shaker incubator at 45°C adjusted to 100 rpm until the complete evaporation of the water content, and then dried AgO-NPs were grinded using mortar for the radiograph diffraction (diffractometer system=EMPYREAN, NRC) (42 kV/120 mA) with CuK radiation, using Ka of the Cu (k=1.542 Å), and the sweep was conducted between 10° and 80°.

The LD_{50} of silver oxide nanoparticles

For determining the LD_{50}, a pilot dosing rate of 2000 mg/kg body weight (BW) caused 100% mortality within less than 48 h. Female albino mice (N=36) were distributed equally into six groups and administered orally per kg of BW by 100, 200, 400, 600, 800, and 1000 mg doses. LD_{50} of AgO-NPs was calculated by determining the dose that caused half number of each group mortalities (50%) of the mice. After administration, the skin and fur changes, eye secretion, and respiration and behavior patterns of the mice were observed. Special attention was paid on the clinical signs of toxicity, including tremors, convulsions, salivation, nausea, vomiting, diarrhea, lethargy, coma, and skin hypersensitivity.

The long administration (chronic toxicity) of silver oxide nanoparticles

For determining the chronic toxicity of the prepared AgO-NPs, female Sprague-Dawley rats (BW: 150–200 g) were purchased from the animal house of NRC and kept under uniform environmental conditions. Female Sprague-Dawley rats (N=32) were randomly divided into four groups. The control group (N=8) received no treatment. The high-dose AgO-NPs group (N=8) received 40.0 mg/kg BW (1 : 20 LD_{50}) orally for 30 days. The moderate-dose group (N=8) received 30.0 mg/kg BW (1 : 26.67 LD_{50}) orally for 30 days. The low-dose group (N=8) received 20.0 mg/kg BW (1 : 40 LD_{50}) orally for successive daily 4 weeks by oral gavage. BW was determined before the starting and at the end of the experiment. Random blood samples were collected before starting any dosing rate. Blood samples were collected at the end of the experiment. Harvested blood sera were stored at −20°C until performing the biochemical clinical analysis and assaying ovarian hormones (estradiol and progesterone). Total antioxidant capacity (TAC), catalase (CAT), total proteins, albumin, aspartate aminotransferase (AST), alanine aminotransferase (ALT), creatinine, alkaline phosphatase (ALP), haptoglobin (HP), interferon γ, and nitric oxide (NO) were measured in blood sera.

The antimicrobial effect of the plant extract and the prepared silver oxide nanoparticles

E. coli (ATCC 35218) suspension was adjusted by comparison to 0.5 McFarland turbidity standards (5×10^6 cells/ml). The bacterial strains were enriched on selective broth for bacterial propagation [25]. A separate tube containing 40 μl of plant extract and AgO-NPs was added with 0.20 μl/10 ml from enriched broth of each propagated *E. coli* [26]. These tubes were incubated at 37°C for 24 h. The growths of control bacterial strains as well as inhibitions of the bacterial growth due to mixing with plant extract, AgO-NPs, and ciprofloxacin (5 μg) antibiotics were measured by turbidity at 420-nm wavelength. The mean values of inhibition were calculated from the mean of the triple reading in each test.

Preparation of bacterial isolates for the induction of uterine infection in rats and its isolation after induction of endometritis

The bacterial isolates were incubated in 10-ml brain heart infusion broth (Sigma aldrich, 48 Sitnyakovo Blvd., Serdika Offices, 6th fl. Sofia 1505. Bulgaria) overnight at 37°C. The final bacterial dose was adjusted to be 10^6 colony forming unit in 100 μl. All uterine samples were collected using vaginal swabs

moistened with phosphate buffer saline and then were incubated in 10 ml of brain heart infusion broth (Sigma) overnight at 37°C. After incubation, the broth samples were streaked on MacConkey agar and EMB agar media [27].

Animals and experimental design for the induction of endometritis

For determining the therapeutic effect of AgO-NPs *in vivo* after inducing endometritis by inoculating *E. coli* intrauterine, female Sprague-Dawley rats (BW: 170–210 g) were purchased from the animal house of NRC and kept under uniform environmental conditions. Rats (*N*=24) were divided into four groups. The control group (*N*=6) received no treatment. The *E. coli* group (*N*=12) was administered with 100 µl of *E. coli* (10^6 CFU) intrauterine for two successive days (day 0 and day 1). Group 3 (*N*=6) rats received AgO-NPs intrauterine and 100 µl of the prepared AgO (10 mg/head equivalent to 50.0 mg/kg BW). *E. coli* was cultured overnight in 10 ml of brain heart infusion broth (Difco Laboratories, Detroit, Michigan, USA) at 37°C. The bacteria were then diluted in brain heart infusion broth media and grown for 1 h to mid-logarithmic phase. The suspension was centrifuged for 10 min at 5000 *g* and was washed in normal saline. The optical density was measured, and the bacteria samples were adjusted to the desired concentrations. The final *E. coli* preparation contained 5×10^6 CFU in 0.50 ml of normal saline [28]. On day 6, inoculated rats (*N*=12) were subjected to blood sampling for clinical biochemical assaying and vaginal swabs were obtained and strained with Wright stain to identify the presence of neutrophils and confirm the establishment of endometritis. Half (*N*=6) of the inoculated rats and the control rats were subjected to euthanasia for performing histopathological studies. The ovaries, uterus, liver, kidney, and spleen were preserved in formalin 10%. Blood samples were collected from all rats before euthanasia. On day 6 and day 7, rats of the other half of the induced endometritis group (*N*=6) and AgO-NPs group (*N*=6) were inoculated with 100 µl of the prepared AgO (10 mg/head) intrauterine. On day 12 (5 days after treatment with silver), treated rats were weighted, and uterine swabs were smeared and stained with Wright stain. Blood samples were collected and their ovaries, uteri, livers, and kidneys were preserved in formalin 10%.

The harvested blood sera were stored at −20°C and were subjected to the biochemical clinical analysis of ovarian hormones (estradiol and progesterone), TAC, CAT, total proteins, albumin, AST, ALT, creatinine, ALP, HP, lipid peroxide product [malondialdehyde (MDA)], and NO.

Histopathological examination

Selected tissues (ovaries, uteri, livers, and kidneys) were fixed in formalin solution (10%), followed by dehydration in different concentrations of alcohol, and then embedded in paraffin, sectioned at a thickness of 4–5 µ, and stained with hematoxylin and eosin. The tissue sections were examined and photographed with the camera of Olympus light microscope (Olympus BX 51, Tokyo, Japan) [29].

Statistical analysis

Data was subjected to statistical analysis using IBM SPSS statistical software version 20.0 (2011) using simple one-way analysis of variance to determine the effect of the treatments on the studied parameters. Duncan's multiple range test was used to differentiate between means.

Results

The characterization of the prepared silver nanoparticle

The prepared AgO-NPs are spherical in shape as observed on the TEM (Fig. 1a). The size of AgO-NPs ranged from 3.54 to 28.05 nm (average 12.87 nm). The crystal structure of AgO-NPs determined by using XRD showed a similar size of the particles as in TEM analysis (Fig. 1b).

Antimicrobial susceptibility of the isolated *Escherichia coli*

The *E. coli* recovered from mares with endometritis showed a broad and variable antimicrobial resistance profile with complete resistance (100%) against amoxicillin/clavulanic acid, ampicillin, ciprofloxacin, tetracycline, gentamicin, and trimethoprim-sulfamethoxazole, followed by amikacin (91%), cephalothin (72.7%), cefotaxime (63.6%), ceftazidime (54.6%), and cefazolin (45.5%). Moreover, 36.4% resistance was observed against cefoxitin, cefepime, imipenem, and chloramphenicol.

Determination of LD_{50} of silver oxide nanoparticles

The pilot dose of 2000 mg/kg BW caused 100% mortalities. The doses started from 1000 mg/kg BW in descending order until reaching 100 mg/kg BW in six doses. Using 1000 mg/kg BW in female mice caused 66.67% mortalities with the presence of red spots on the skin. The 800 mg/kg BW dose of AgO-NPs caused 50% mortalities in female mice. The 600 mg/kg BW dose caused 33.33% mortalities with the presence of red spots on the skin, whereas the use of

Figure 1

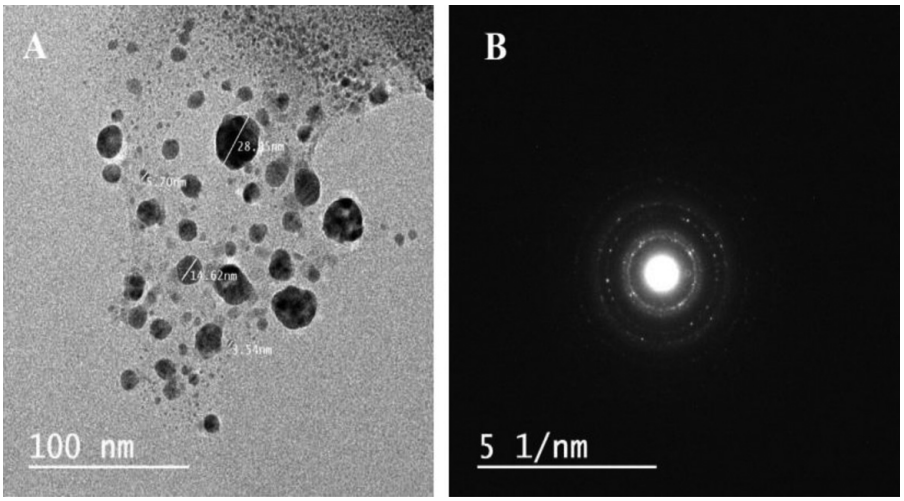

The shape and size of the AgO-NPs (a) and the crystallinity of the AgO-NPS (b) determined by transmission electron microscope (TEM). AgO-NPs, silver oxide nanoparticles.

Figure 2

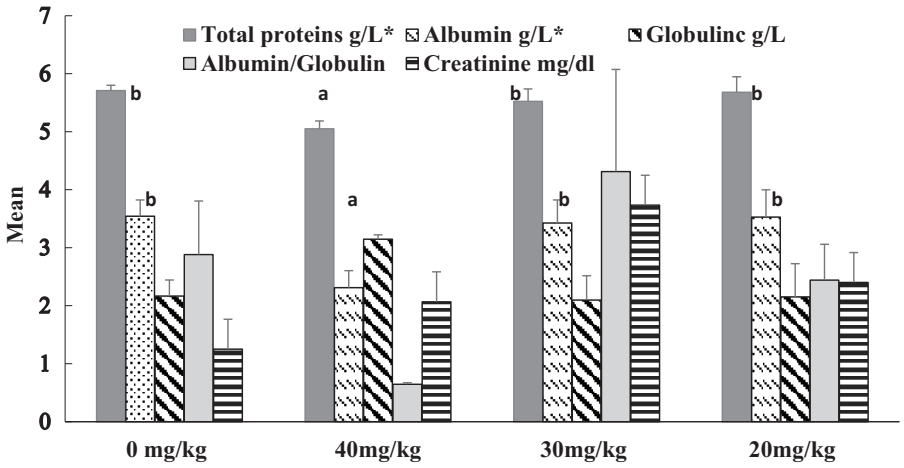

Effect of three doses of AgO-NPs (20, 30, and 40 mg/kg body weight) on total proteins, albumin, globulin, albumin/globulin ratio, and creatinine. Different superscripts (a, b) are significant at *P* value less than 0.05; *significant at *P* value less than 0.05. AgO-NPs, silver oxide nanoparticles.

the dose of 400 mg caused 16.66 mortalities with red spots on the skin. The single-dose administration of 100 or 200 mg/kg BW was safe and did not cause any mortality.

Blood biochemical changes in rats treated with 20, 30, and 40 mg/kg body weight silver oxide nanoparticles for 4 weeks

The total proteins and albumin have decreased in rats treated with 40 mg/kg BW of AgO-NPs compared with the control and other treatments (Fig. 2). Creatinine insignificantly increased in all treated groups compared with the control one. ALP, AST, and ALT showed no significant changes in all rats treated with different doses of AgO-NPs compared with the control group (Fig. 3). Neither total cholesterol nor triglycerides changed in all rats treated with different doses of AgO-NPs compared with controls (Fig. 4). Estradiol (E2) decreased ($P<0.01$) in rats treated with 30 and 40 mg/kg BW AgO-NPs, with increased ($P<0.05$) progesterone (P4) in all treated groups in comparison with controls (Fig. 4).

Both control rats and those treated with 20 mg AgO-NPs showed no change in their BW (Table 1). However, treatment of rats with 30 and 40 mg/kg BW decreased their BWs ($P=0.005$). All treatments of AgO-NPs increased HP ($P=0.019$) but did not change interferon γ, TAC, glutathione-S-transferase (G-S-T), and MDA concentrations. CAT activity

Figure 3

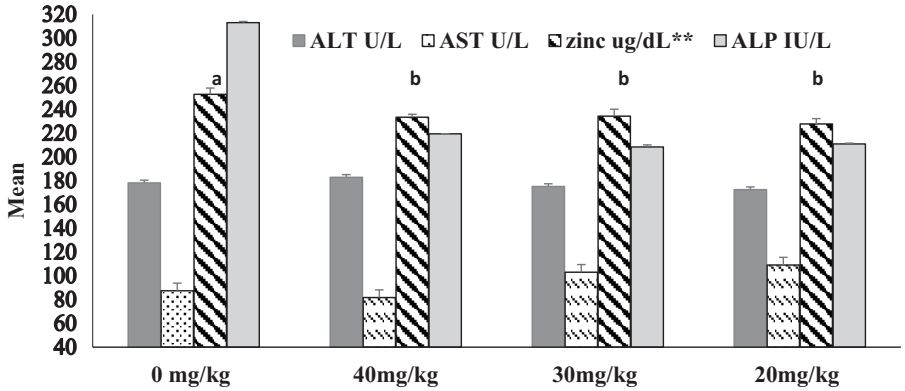

Effect of three doses of AgO-NPs (20, 30, and 40 mg/kg body weight) on AST, ALT, ALP, and zinc. Different superscripts (a, b) are significant at *P* value less than 0.05; **significant at *P* value less than 0.01. AgO-NPs, silver oxide nanoparticles; ALP, alkaline phosphatase; ALT, alanine aminotransferase; AST, aspartate aminotransferase.

Figure 4

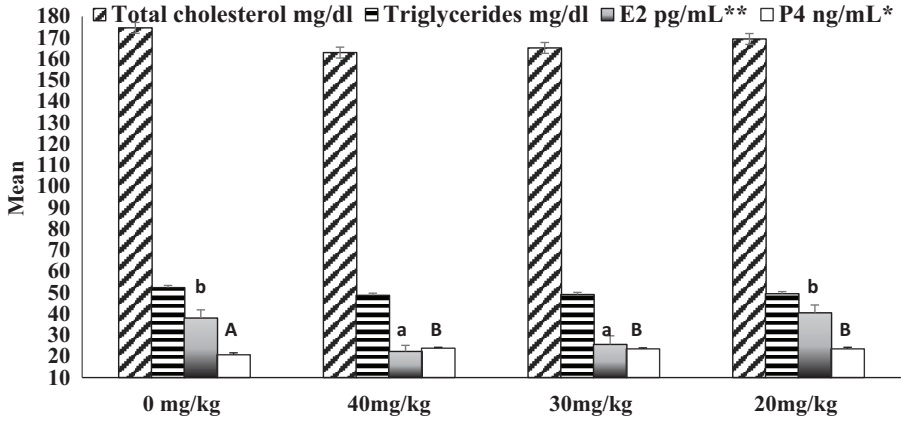

Effect of three doses of AgO-NPs (20, 30, and 40 mg/kg body weight) on total cholesterol, triglycerides, E2, and P4; **significant at *P* value less than 0.01; *significant at *P* value less than 0.05. Different superscripts (A, B) for progesterone and (a, b) for E2 are significant at *P* value less than 0.05. AgO-NPs, silver oxide nanoparticles.

Table 1 Mean±SEM body weight, oxidants, and antioxidants parameters in female rats treated with three different doses of silver oxide nanoparticles for 30 days

	AgO-NP treatments				
Parameter	0.0 mg	20 mg	30 mg	40 mg	*P* value
Initial BW (g)	175.00±5.25^{ab}	168.63±4.43^{a}	185.25±3.53^{b}	180.25±3.53^{ab}	0.037
Final BW (g)	175.00±5.24^{b}	167.14±4.31^{ab}	160.38±4.14^{a}	165.00±4.40^{ab}	.215
BW change%	0.00±.00^{b}	−0.89±4.24^{b}	−13.44±1.37^{a}	−8.31±2.48^{ab}	0.005
HP (mg/dl)	14.42±7.16	21.11±3.13	33.89±3.09	29.05±2.69	0.019
Interferon γ (pg/ml)	101.86±4.64^{b}	98.57±9.51^{a}	99.87±6.64^{b}	98.22±11.62^{a}	0.99
MDA (nmol/ml)	9.97±0.03	9.84±.11	9.46±.17	9.91±0.06	0.002
NO (μmol/l)	47.69±1.27	38.15±.99	39.05±1.56	35.49±1.04	0.0001
TAC (mM/l)	0.19±0.02	0.26±0.06	0.20±0.05	0.27±0.03	0.309
GSH (mg/dl)	37.86±.76	50.04±8.15	36.14±1.07	45.86±3.61	0.053
G-S-T (U/l)	3733±93	3573±419	4066±228	4107±206	0.308
Catalase (U/ml)	65.82±10.14	99.53±17.01	107.75±25.71	119.57±9.13	0.041

AgO-NP, silver oxide nanoparticle; BW, body weight; GSH, reduced glutathione; G-S-T, glutathione-S-transferase; HP, haptoglobin; MDA, malondialdehyde product; NO, nitric oxide; TAC, total antioxidant capacity. Means with different superscripts (a, b, c) are significantly different at *P* value less than 0.05.

increased (P=0.041) in all rats treated with different doses of AgO-NPs compared with the control. The three doses of AgO-NPs declined NO (P=0.001), but the doses of 20 and 40 mg AgO-NPs increased reduced glutathione (GSH) (P=0.053; Table 1). Zinc was significantly increased (P<0.01) in all treated rats (Fig. 2).

In vitro antibacterial effect of silver oxide nanoparticles on *Escherichia coli* and its isolation from *in vivo* induced endometritis

Both AgO-NPs and tetracycline inhibited (P<0.0001) the growth of *E. coli* compared with either the thymus plant extract or the normal nontreated bacterial growth (Fig. 5). The rats inoculated with *E. coli* in their vagina showed bacterial growth compared with the untreated groups (control and AgO-NPs).

Blood biochemical changes in rats inoculated with *Escherichia coli* and treated with silver oxide nanoparticles after infection

Although the initial BW tended (P>0.05) to be high in all treated groups, the final (P<0.05) BW change declined in rats treated with *E. coli* but increased in the two AgO-NP-treated groups. The BW change %

Figure 5

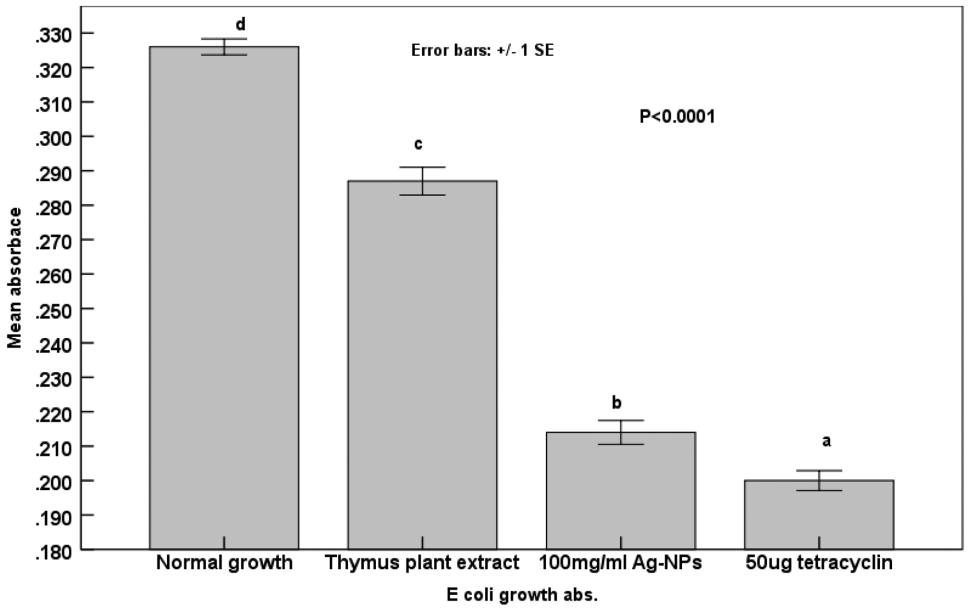

The *in vitro* antibacterial effect of silver nanoparticles (100 mg/ml) on the *Escherichia coli* growth absorbance (abs.) with error bars.

Table 2 Mean±SEM of body weight/g and uterine weight/g, blood proteins, liver and kidney functions in rats experimentally inoculated with *Escherichia coli* intrauterine and treated with silver oxide nanoparticles

			Escherichia coli-induced endometritis		
Treatment	Control	AgO-NPs	No treatment	AgO-NPs	*P* value
Initial BW (g)	169.75±1.65^{a}	187.33±7.21^{ab}	184.67±9.24^{ab}	196.00±8.08^{b}	0.084
Final BW (g)	169.25±1.49^{a}	193.00±3.78^{b}	180.67±4.09^{ab}	198.33±10.80^{b}	0.017
BW change %	−0.29±0.29	3.39±5.21	−1.89±2.72	1.66±7.77	0.855
Ut. weight (g)	0.88±0.12^{a}	1.24±0.18^{ab}	1.66±0.13^{b}	0.94±0.23^{a}	0.082
Relative Ut. W	0.53±0.12^{a}	0.64±0.10^{ab}	0.90±.09^{b}	0.49±0.13^{a}	0.104
Haptoglobin (mg/dl)	14.42±7.16	19.47±1.89	20.84±5.12	30.94±4.91	0.272
Total proteins (g/l)	5.71±0.11^{b}	4.48±0.19^{a}	4.34±0.21^{a}	4.87±0.11^{a}	0.0001
Albumin (g/l)	3.54±0.08^{b}	1.95±0.15^{a}	2.34±0.07^{ab}	2.43±0.25^{ab}	0.010
Globulin (g/l)	2.22±0.18	2.54±0.32	2.00±0.18	2.44±0.28	0.744
Alb./Glo.	2.88±0.06	0.81±0.16	1.19±0.11	1.05±0.25	0.220
Creatinine (mg/dl)	0.58±.17^{a}	1.05±0.34^{ab}	0.57±0.16^{a}	1.24±0.13^{b}	0.004
AST (U/l)	116.50±11.21^{ab}	100.85±14.46^{a}	180.55±21.32^{b}	178.86±3.12^{b}	0.022
ALT (U/l)	96.93±3.14^{b}	96.73±0.72^{b}	85.97±2.01^{a}	95.04±3.39^{b}	0.047
ALP (IU/l)	313.06±46.49^{b}	103.75±0.75^{a}	106.52±1.34^{a}	106.69±2.35^{a}	0.027

AgO-NPs, silver oxide nanoparticles; ALT, alanine aminotransferase; Alb./Glo., albumin/globulin ratio; ALP, alkaline phosphatase; AST, aspartate aminotransferase; BW, body weight; Ut. W, uterine weight. Means with different superscripts (a, b) are significantly different at *P* value less than 0.05.

Table 3 Mean±SEM of total cholesterol (mg/dl), triglycerides (mg/dl), and ovarian hormones in rats experimentally inoculated with *Escherichia coli* intrauterine and treated with silver oxide nanoparticles

			Escherichia coli-induced endometritis		
Treatment	Control	AgO-NPs	No treatment	AgO-NPs	*P* value
T. cholesterol (mg/dl)	174.56±4.26	186.25±24.41	171.47±0.96	201.60±29.14	0.494
Triglycerides (mg/dl)	52.34±1.49	46.09±.61	48.55±1.00	52.21±2.08	0.057
E2 (pg/ml)	46.77±6.38^{b}	14.94±1.65^{a}	14.68±4.85^{a}	26.27±5.59^{ab}	0.011
P4 (ng/ml)	22.63±1.09	23.04±.75	21.74±1.50	23.51±1.03	0.163

AgO-NPs, silver oxide nanoparticles; E2, estradiol; P4, progesterone; T, total. Means with different superscripts (a,b) are significantly different at *P* value less than 0.05.

Table 4 Mean±SEM body weight/g, oxidants, and antioxidants parameters in female rats treated with silver oxide nanoparticles

			Escherichia coli-induced endometritis		
Treatment	Control	AgO-NPs	No treatment	AgO-NPs	*P* value
MDA (nmol/ml)	9.98±0.01	9.95±0.01	9.98±.02	9.99±0.01	0.322
NO (μmol/l)	47.69±1.27^{b}	38.43±1.40^{a}	43.89±1.11^{ab}	43.87±1.95^{ab}	0.016
TAC (mM/l)	0.19±.03	0.14±0.01	0.23±0.09	0.15±0.04	0.622
GSH (mg/dl)	37.86±.76^{a}	36.24±0.71^{a}	44.37±2.32^{b}	36.44±1.21^{a}	0.005
Catalase (U/l)	59.84±9.06^{ab}	82.17±20.47^{b}	29.46±4.11^{a}	88.89±22.89^{ab}	0.231
G-S-T (U/l)	3498±76^{ab}	3998±300^{ab}	4653±663^{b}	3515±110^{a}	0.042
Zinc (μg/dl)	254.26±5.12^{b}	234.63±2.73^{a}	246.85±2.45^{b}	227.22±2.78^{a}	0.002

AgO-NPs, silver oxide nanoparticles; GSH, reduced glutathione; G-S-T, glutathione-S-transferase; MDA, malondialdehyde product; NO, nitric oxide; TAC, total antioxidant capacity. Means with different superscripts (a, b, c) are significantly different at *P* value less than 0.05.

of inoculated rats with *E. coli* showed insignificant decrease compared with controls, AgO-NPs, and AgO-NPs after induction of endometritis (Table 2). Both uterine weight ($P>0.05$) and the relative uterine weight increased in the *E. coli*-treated groups either treated or not treated with AgO-NPs.

HP insignificantly increased in rats treated with AgO-NPs, *E. coli*-induced endometritis, and AgO-NPs treatment after inducing endometritis with *E. coli* (Table 2). Compared with controls, all treatments showed decreased total proteins ($P=0.0001$) and albumin ($P=0.024$). AgO-NPs increased creatinine ($P=0.004$). The *E. coli* groups treated and nontreated with AgO-NPs showed increased AST ($P=0.022$; Table 2). ALP decreased ($P=0.027$) in all treated groups.

E. coli and AgO-NPs decreased ($P=0.011$) estradiol concentrations compared with controls (Table 3). Treatment with AgO-NPs and endometritis induced by with *E. coli* decreased NO ($P=0.016$; Table 4). The two treatments of AgO-NPs did not affect GSH but the induced endometritis with *E. coli* increased it ($P=0.005$). The activity of G-S-T has been increased after inducing endometritis with *E. coli*, thought rats treated with AgO-NPs showed slight increase ($P=0.042$). A slight decrease ($P=0.002$) of zinc was observed in AgO-NP-treated groups (Table 4).

The vaginal cytology

The vaginal swabs collected seven days after inoculation of rats with *E. coli* indicated the presence of polymorphonuclear cells, where more than 1% polymorphonuclear cell threshold level on ROC curve on confirmed the development of endometritis to indicate the presence of inflammatory cells (Fig. 6).

The histopathological changes in experimentally induced endometritis in rats

Histopathological examination of ovary in control and AgO-NP-treated rats showed normal and preserved ovarian architecture (Fig. 7a, b), whereas rats infected with *E. coli* showed severe diffuse hemorrhage along the ovarian tissues. Most of the examined sections revealed severe multifocal leukocytic cell infiltrations associated with severe degeneration of the lining epithelium (Fig. 7c). The examined ovarian section in induced endometritis and treated with AgO-NPs (combination group) showed variable degrees of improvement with mild congestions as compared with that of the *E. coli*-infected group (Fig. 7d).

The uterine tissue in control and AgO-NPs-treated rats revealed normal uterine histological structures (Fig. 8a,b). However, the infected group with *E. coli* showed severe diffuse submyometrial congestions and hemorrhages (Fig. 8c). In addition, uterine sections of the *E. coli*-infected rats revealed severe multifocal

Figure 6

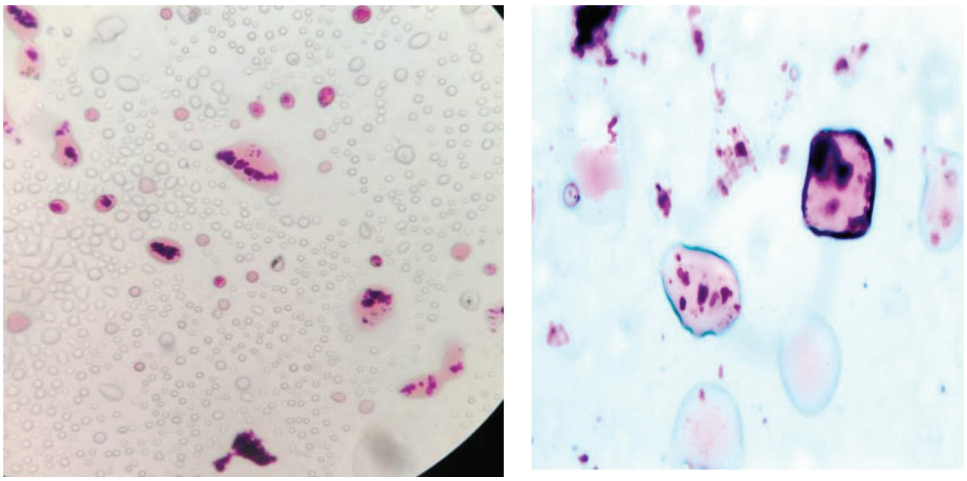

The development of endometritis is confirmed by the vaginal swab stained by the Wright's stain to indicate the presence of inflammatory cells.

Figure 7

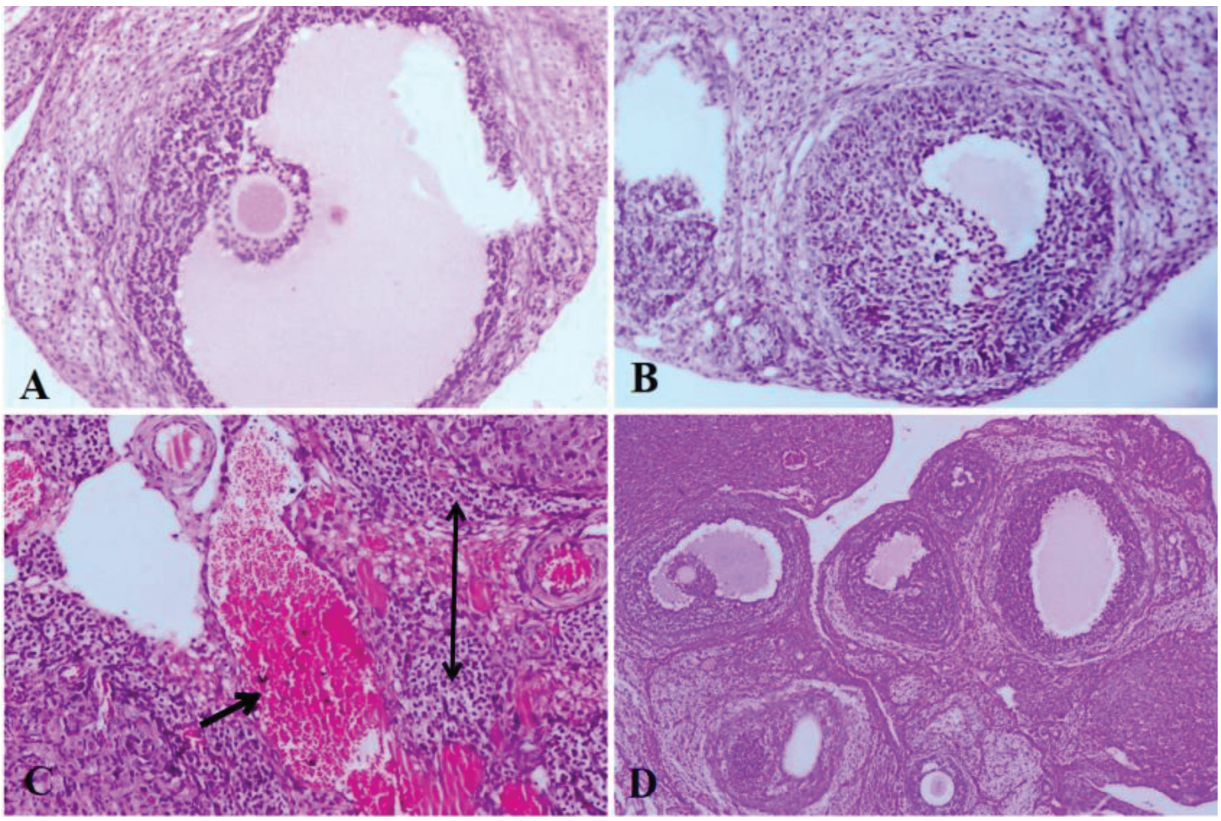

Photomicrograph of ovarian tissue sections stained with H&E (×100) showing normal histological picture in the control (a), normal histological picture of Ag-treated rats (b), *Escherichia coli*-treated rats showing severe hemorrhage (arrow) and severe leukocytic cell infiltrations (double headed arrow) associated with severe degeneration of the lining epithelium (c), and Ag and *E. coli*-treated group showing marked improvement and restoration of the normal histologic picture with mild congestions (d).

polymorphonuclear cell aggregation associated with severe epithelial and glandular cells vacuolization (Fig. 8c). The uterine section in treated *E. coli*-induced endometritis group (Fig. 7d; *E. coli*+AgO-NPs) showed variable degrees of improvement with mild congestions and mild vacuolization as compared with that of the *E. coli*-infected group (Fig. 8d).

The liver tissue in control and AgO-NPs-treated rats showed normal and preserved hepatic architecture

Figure 8

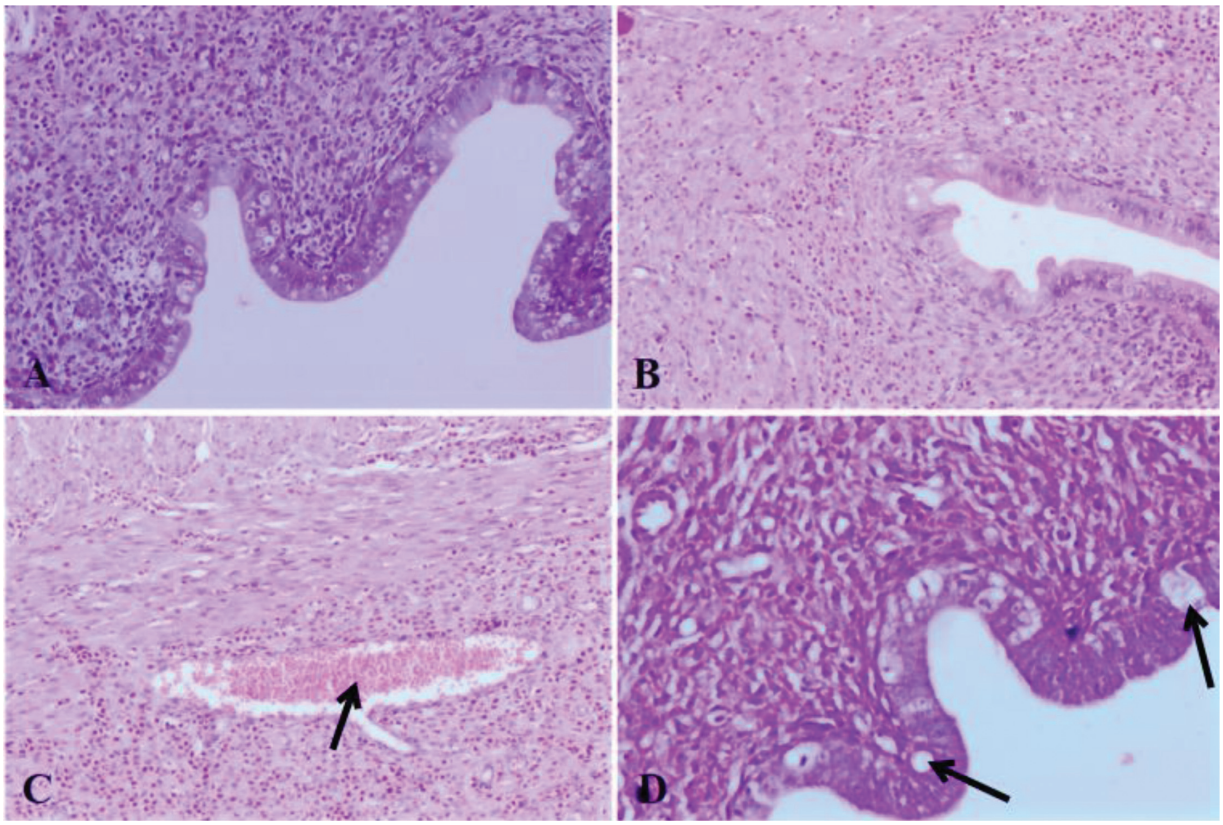

Photomicrograph of uterine tissue stained with H&E (×100) showing normal histological picture in the control (a), normal uterine histological picture with mild leukocytic cell infiltration of Ag-treated rats (b), *Escherichia coli*-treated rats showing severe hemorrhage (arrow) and submyometrial congestions (c), and uterine tissue of Ag and *E. coli*-treated group were apparently healthy with mild vacuolar degenerations (d, arrows).

(Fig. 9a, b), whereas the rats infected with *E. coli* showed severe congestion of central, portal veins, and hepatic sinusoids associated with hemorrhages within hepatic parenchyma. Focal areas of mononuclear inflammatory cell aggregations were also noticed in some examined sections as well as edema and hyperplasia in portal area, and proliferation of biliary epithelium (Fig. 9c). The examined hepatic section of *E. coli*+AgO-NP treatment group were seen to have normal structure (Fig. 9d).

The kidney in control and AgO-NPs treated rats were seen to have normal renal architecture (Fig. 10a, b). Histopathological examination of kidney in infected rats with *E. coli* showed severe congestion and marked hyperemia of the renal blood vessels associated with severe inflammatory cell infiltrations mainly lymphocytes and neutrophils. Some examined sections showed interstitial hemorrhage and other sections showed severe degeneration of the epithelial lining of the renal tubules, and renal cast formation was observed (Fig. 10c). Renal sections in *E. coli*+ AgO-NPs were apparently healthy with mild degeneration of epithelial lining of renal tubules (Fig. 10d).

Discussion

This study synthesized AgO-NPs using the green method (aqueous extract of thymus plant). In white albino rats, the intraperitoneal single-dose administration of 4000 mg/kg BW resulted in higher LD_{50} with no mortality than that observed in the current experiment using female mice [30]. This higher LD_{50} previously recorded was related to the higher size of the prepared AgO-NPs [31], as the increase in the size of AgO-NPs from 25 to 35 nm increased the LD_{50} from 250 to 350 mg/kg BW [31]. In contrast to our results, AgO-NPs showed lower LD_{50} of 280 mg/kg BW [31,32].

In vitro, the toxic effects of AgO-NPs are dependent on the exposure dose, the cell type, the particle size, and the exposure time rather than the surface coating, but *in vivo*, they are deposited in spleen, liver, and kidneys, induce pancreatic toxicity, and cause hepatic inflammation [33]. The use of 20 mg/kg BW orally

Figure 9

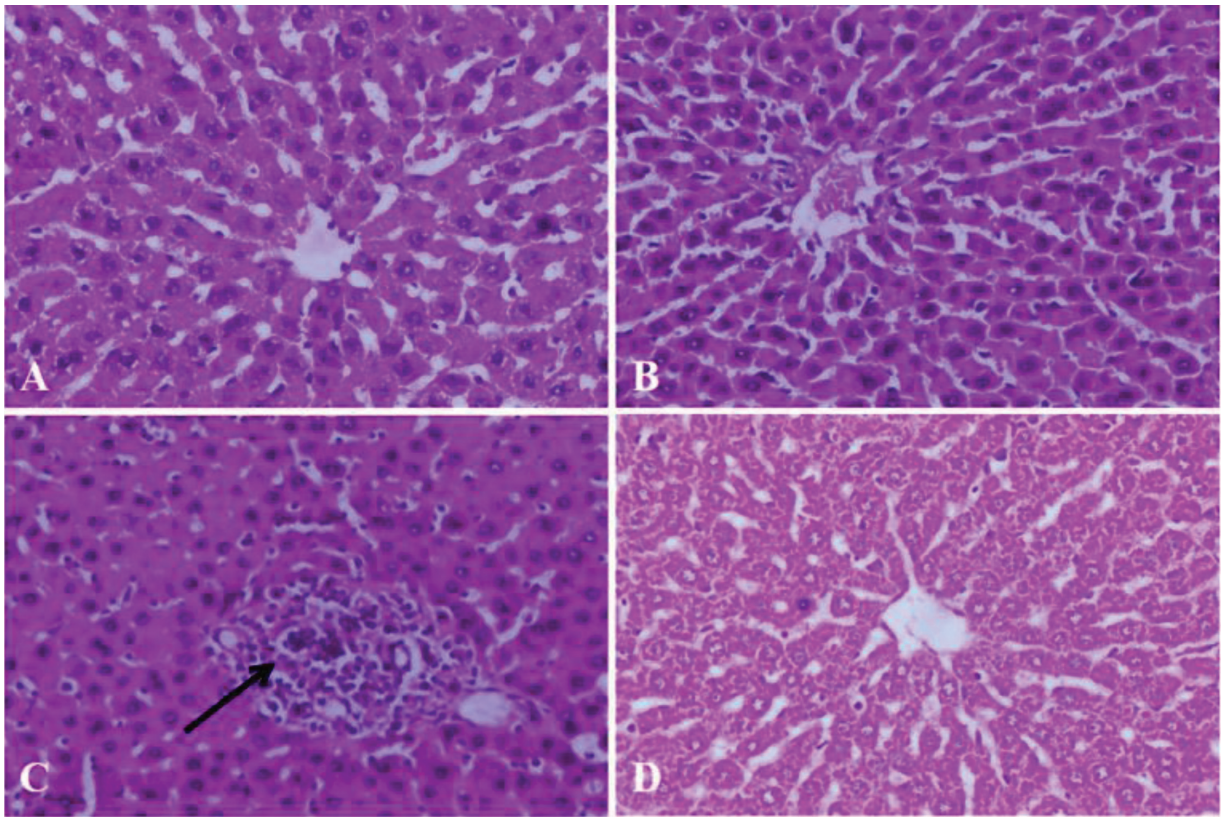

Photomicrograph of hepatic tissue sections stained with H&E (×200) showing normal histological picture in the control (a), normal histological picture with mild congestion and hydropic degeneration of Ag-treated rats (b), *Escherichia coli*-treated rats showing focal area of mononuclear inflammatory cells infiltrations (arrow) associated with focal coagulative necrosis (c), and Ag and *E. coli*-treated group showing obvious regeneration of the normal histologic picture with mild degeneration of hepatocytes (d).

in our female rats for 30 days did not alter the BW but the use of 30 and 40 mg/kg BW reduced it. Similarly, male rats treated orally with doses higher than that used in the current study (100 mg/kg BW AgO-NPs) for the same interval showed significant changes in their BW [32]. The insignificant effect of all doses of AgO administered orally to female rats of this study on ALT and AST reflects no liver damage. There was elevation of ALT and AST and the liver damage was low in animals treated with 25 nm AgO-NPs compared with 35 nm AgO-NPs, indicating size-dependent toxic effects [31]. Similar to our results, the use of 100, 200, and 300 ppm, which are equivalent to 1.0, 2.0, and 3.0 mg AgO-NPs administered via intraperitoneal injection in rats for 3 weeks, did not alter neither BW nor organ coefficients but altered the redox status of liver, kidney, and spleen [34].

In contrast to the significant increase of HP in female rats of this study, male rats treated orally with 100 mg/kg BW AgO-NPs for 4 weeks showed a slight nonsignificant increase [32]. Compared with the control treated female rats of this study, interferon γ did not vary, which indicates the safety of our three doses, where the cytotoxic effect of nanosilver appeared at high concentration and the lower concentrations inhibited the cytokine production [35]. In contrast to the female rats treated with 20, 30, and 40 mg/kg BW AgO-NPs, the oral administration of 50 mg/kg BW AgO-NPs to male rats for 79 days increased NO in both lung and heart tissues [36]. Although 20 and 40 mg/kg BW AgO-NPs increased GSH production in female rats of this study, the lung and heart of treated male rats showed lower values [36]. The increases of total antioxidant capacity and CAT in female rats treated with 20, 30, and 40 mg/kg BW AgO-NPs are in contrast to their significant decrease in the heart and lung tissues of male rats [36], indicating that higher dose, the route of administration, the sex, and the longer administration interval reversed the antioxidant properties of AgO-NPs [37], which was recorded in male rats by the decrease of all antioxidants and the increase of oxidative stress markers [36]. The stability of the decrease of reactive oxygen species products MDA and NO and the slight increase or the unchanged antioxidants in female rats of this study confirm that the doses used here and the interval (4 weeks) can be referred to the antioxidant activity of the

Figure 10

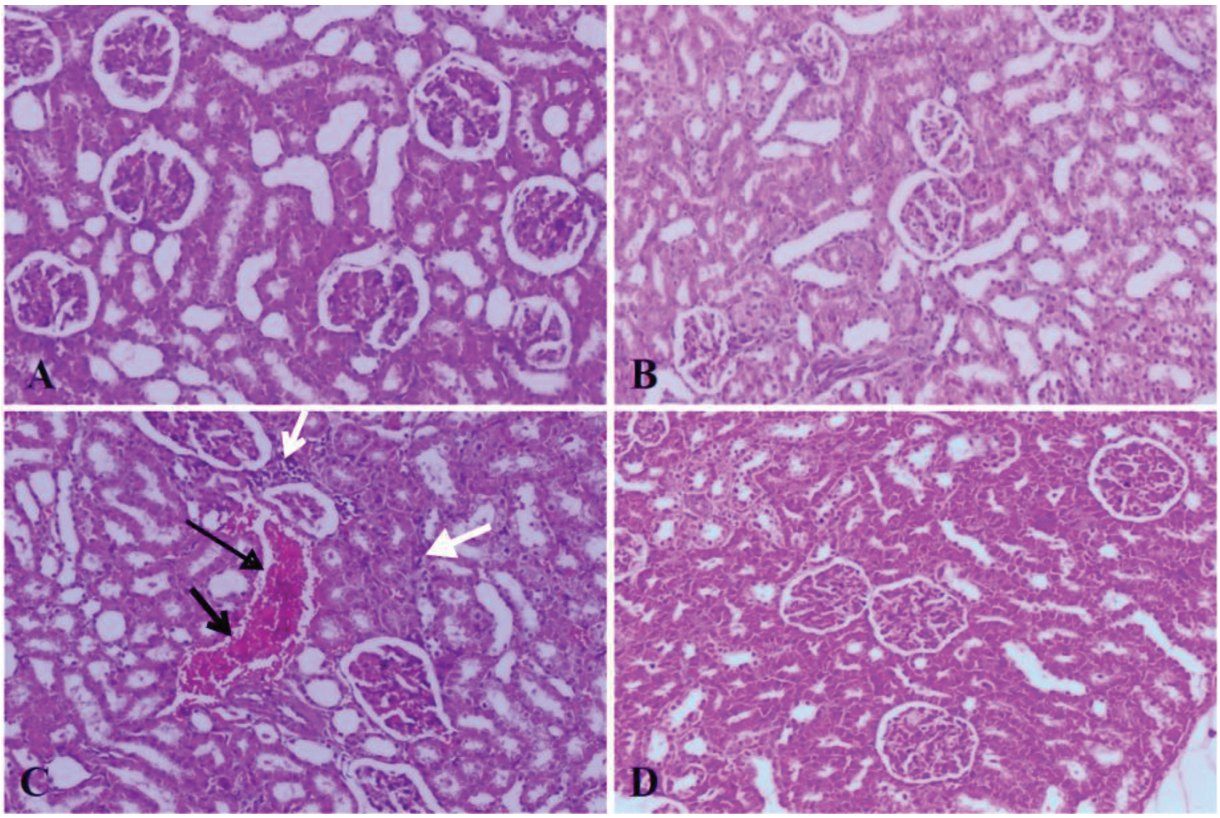

Photomicrograph of renal tissue sections stained with H&E (×100) showing normal histological picture in the control (a), normal histological picture of Ag-treated rats with mild leukocytic infiltrations and degeneration of tubular epithelium (b), *Escherichia coli*-treated rats showing severe hemorrhage (black arrow) and severe leukocytic cells infiltrations in the renal cortex (white arrow) associated with severe degeneration of the lining epithelium (c), and Ag and *E. coli*-treated group showing marked regeneration of the normal histologic picture with mild degeneration of lining epithelium of some renal tubules (d).

synthesized AgO-NPs reported *in vitro* by 2,2-Diphenyl-1-picryl-hydrazyl free radical scavenging activity and the ferric antioxidant deducing power [38]. The antioxidant property of AgO-NPs synthesized by the plant extract was referred to the presence of silver in two oxidation states, Ag+ and Ag2 +, and phytochemicals are capped on the AgO-NP surface [39]. AgO-NPs can be recommended for short therapeutic courses in low concentration because the exposure dose, particle size, exposure time, and surface coating play a role in elaborating its effects [33]. The nonsignificant change of triglycerides and total cholesterol in female rats of this study is in contrast to their increase in the blood plasma of male rats treated for 79 days with 50 mg AgO-NPs [36]. However, the doses used in the current study were higher than that was previously reported, and the lower size of the synthesized AgO-NPs was reported to be the more toxic [40]. Size, shape, roughness, specific surface area, surface energy, charge, zeta potential, surface morphology, crystal structure, and ligands, all of these factors influence the effects of the NPs [41]. The antimicrobial activity of metal NPs is influenced by the properties of any metal NP which depends on the medium composition, pH, osmotic pressure, temperature, irradiation, solubility, aggregation, and surface charge or modification [41]. Similar to female rats of this study, mice that received 0.20 mg of 10.0 nm AgO-NPs showed congestion, vacuolation, single cell necrosis, and focal necrosis in the liver which were not evident following the administration of either 60 or 100 nm, indicating that the smaller size is more toxic [42]. Although the dose of AgO-NPs of the current study did not influence the liver enzymes, a significant increase in AST and an increasing tendency in ALT were observed in mice received intraperitoneally 10 nm AgO-NP compared with 60 and 100 nm [42] and male Sprague-Dawley rats administered single dose orally 20 mg/kg of 7.9 nm AgO-NPs (2 or 20 mg/kg) [43].

Similar to the decreased production of progesterone in our female rats treated with 20, 30, and 40 mg AgO-NPs and the decreased production of estradiol after treatment with 30 and 40 mg/kg BW, the porcine granulosa cells cultured *in vitro* in the presence of

0.1, 1.0, 10.0, or 100 μg/ml AgO-NPs produced more progesterone and low estradiol [44]. When bovine granulosa cells were treated with 10 nm AgO-NPs at various concentrations (1–100 μg/ml) for 24 h, AgO-NP-treated cells suppressed the steroid hormone synthesis, and this suppression was referred to the apoptosis and oxidative stress that changed the pattern of steroid hormone synthesis [45] and the inhibition of cell proliferation observed after exposing human ovarian and colon cancer cell lines to 7.5 nm AgO-NPs after their interaction with the cell membrane proteins and activating the signaling pathways [46]. In contrast, silver nanorods promoted progesterone and estradiol synthesis by the ovarian cells of rats in a time and dose-dependent manner [47]. The decreased estradiol concentrations reported in the current study was also reported in female rats treated with 0.5, 1.0, and 5.0 mg/kg AgO-NPs via intraperitoneal injection for 35 days and referred this decrease to the follicular atresia [48]. Although female rats of this study did not present any change in TAC and MDA but female rats treated with 0.5, 1.0, and 5.0 mg/kg AgO-NPs via intraperitoneal injection for 35 days showed reduced TAC and SOD levels and elevated MDA content indicating that not only size and dose of NPs but also the route of admirations and the longer the exposure time are important in enhancing the toxic effects [48]. So, the low dose of AgO-NPs (20 mg/kg BW) can be recommended for longer therapeutic purposes with minimal effects on the fertility.

The adverse effects of the induced *E. coli* intrauterine infection are usually attributed to its endotoxin production. Either the bacteria or the bacterial LPS was used to induce endometritis in mice [4,49] and rats [50]. In agreement with our results, the induction of bacterial endometritis increased the uterine absolute and relative weights in treated and nontreated groups compared with the control one after the surgical inoculation of two different bacterial isolates into the uteri ligated at the cervix [50]. Experimentally induced endometritis after the injection of *E. coli* in rats previously treated with progesterone for 5 days was confirmed by the increased uterine diameter [51]. The detection of polymorphonuclear cells in the stained vaginal swabs taken from rats of our study was also observed after the uterine flushing collected from rats surgically inoculated with *E. coli* and *S*taphylococcus *aureus* [50]. In agreement with the experiment of Tiwari *et al.* [50], the inoculated *E. coli* was re-isolated from the induced endometritis before starting the treatment with AgO-NPs.

Similar to our results, the uteri of rats inoculated with *E. coli* and *S. aureus* revealed intensive infiltration of inflammatory cells in the submucosa, considerable thickening of the mucosa, along with heavy infiltration of inflammatory cells, whereas the treated animals showed serosal congestion and dilated submucosal glands with lower number of inflammatory cells [50]. When endometritis was induced in mice using bacterial LPSs, the uterine epithelial shedding of epithelial cells and the abundance of inflammatory cells were recorded [51]. Hyperemia, hemorrhage, shedding of epithelial cells, and multiple inflammatory (polymorphonuclear) cells that had infiltrated the uterine tissues were seen in rats subjected to endometritis using LPS [4]. Although AgO-NPs were administered intrauterine, adverse pathological and clinical biochemical analyses were noticed in the liver and kidney, which agree with the reported accumulation of AgO-NPs administered *in vivo* in the local and distant organs and its capability to cross different biological barriers and enter the systemic circulation [52]. The mild leukocytic infiltration noticed in the uteri of AgO-NPs group could be referred to the induction of uterine inflammation and the production of oxidative stress at the site of exposure [52,53]. The accumulation of AgO-NPs in the mice endometrium increased the interleukin production [54] and caused inflammatory lesions in lungs of Sprague-Dawley rats [55,56]. The inflammation of the kidney in our rats administered AgO-NPs intrauterine agreed with their accumulation in female kidneys more than those of males [57]. Similar to the inoculation of *E. coli* intrauterine for the development of chronic endometritis in rats of this study, LPS acute model of inducing mouse endometritis resulted in damage of the uterine tissue, hyperemia, hemorrhage, shedding of epithelial cells, congestion, edema, and irregular shape [58]. Rabbits administered *E. coli* and *S. aureus* isolated from cows showed detached endometrial epithelial cells with visible inflammatory exudates and blood spots between intercellular spaces [3]. AgO-NPs administered intrauterine in the treated rats of our study attenuated and alleviated the presence of inflammatory cells infiltrates, hyperemia, hemorrhages, and shedding of epithelial cells similar to the baicalin flavonoid actions on rabbits [3]. The therapeutic effect of AgO-NPs in the treatment of endometritis induced by *E. coli* in the current work was also reported when Irisin [58], Resveratrol [59], and Thymol [60] mitigated the adverse effects of either *E. coli* or LPS models of inducing endometritis via AMPK/NF-κB or NF-κB signaling pathways.

The insignificant decrease in progesterone in rats inoculated with *E. coli* in our experiment was noticed from day 11 to day 18 in heifers inoculated with *E. coli* after treatment with progesterone to mimic diestrus and ensure elevated circulating P4 at the time of bacterial infusion for 7 days [61] and also decreased in gilts from day 8 after inoculating *E. coli* intrauterine [62]. Similar to the significant decrease of estradiol in our rats treated with either AgO-NPs or *E. coli* and its insignificant decrease in the *E. coli*-AgO-NPs group, rats treated with progesterone for 5 days before injecting *E. coli* in one uterine horn and treated with resveratrol and marbofloxacin for 14 days showed decreased estradiol [59] which decreased also in gilts from days 15 to 18 after a single intrauterine inoculation of *E. coli* [62]. The decrease in both estradiol and progesterone in animals and the delay in developing estrous in animals with endometritis was referred to the effect of bacterial toxins (LPSs) on the pituitary–ovarian axis function as well as prostaglandin production resulting eventually in anestrus [62]. In agreement with the decrease of HP in intrauterine treated rats with the intrauterine treatment with either AgO-NPs or *E. coli* compared with control and *E. coli*-AgO-NPs groups, heifers subjected to induced endometritis using *E. coli* showed low HP concentrations of the endometritis group on day 0, which increased on days 7 and 13 compared with control [61].

The increase of NO in the tissue homogenate of the uteri of surgically infected rats with mixed *E. coli* and *S. aureus* [50] is in contrast to the unchanged circulating NO in rats of our study. This could be attributed to the development of chronic infection in our experiment, the delayed start of treatment (day 7 after inoculation), or the localized infection within the uterus. In contrast to the significant decrease of blood serum levels of GSH, zinc, and G-S-T and nonchange in MDA and TAC in rats of this study treated with AgO-NPs alone or after development of chronic endometritis, mice treated with LPS for the development of acute endometritis showed high MDA and GSH in the uterine tissue [58]. The damage in rats' ovaries treated with *E. coli* and the disturbances in the ovarian hormones simulate the same effect in bovine where the intrauterine infusion of *E. coli* LPS increased plasma concentrations of PGF2α metabolite, decreased plasma progesterone concentrations, and reduced luteal size [63]. Although the intrauterine infusion of LPS in bovine did not influence the preovulatory follicle size [63], the intrauterine inoculation of *E. coli* in rats of our study disturbed the arrangement of granulosa cells within the antral ovarian follicles, and this could be attributed to the reduction of CYP19A1 expression and estradiol production in bovine granulosa cells due to the binding of LPS to the toll-like receptor-4, CD14, and MD-2 receptor complex, leading to the inability of the ovarian follicle granulosa cells to produce estradiol by the aromatization of androstenedione from the theca cells [64]. *E. coli* bovine model to induce endometritis decreased the number of cleaved oocytes developing to morulae when the oocytes were collected by transvaginal ultrasound-guided ovum pickup on day 24, which correlated inversely with endometrial expression of IL-6 on day 6 [65].

Similar to our results, female mice intraperitoneally injected with *E. coli* CVCC195 at a concentration of absolute lethal dose (LD_{100}) showed foci of hepatocellular necrosis and localized foci of interstitial inflammation in the kidney [66]. In agreement with the increase of AST in rats of this study, the increase in both ALT and AST in the rats treated with LPS indicated hepatocellular damage as presented in the liver pathology [67].

Conclusions

The oral administration of 1/40 LD_{50} (20 mg/kg BW) of AgO-NPs synthesized by the eco-friendly green method is safe with no deleterious effect on the animal health and fertility. AgO-NPs have a therapeutic effect on the *E. coli* model of induced endometritis. AgO-NPs have local inflammatory effects and can pass the body barriers with damaging effects on the liver and kidney functions. Any dose of AgO-NPs that was used in the present study can be recommended for short therapeutic courses.

Acknowledgements

The authors thank the National Research Center for funding the current research, under the grant number (NRC: 12050417).

Authors' contributions: A.M.A. prepared the study design, made the statistical analysis, and wrote the manuscript. E.M.M.F. and S.T.O. performed all the in vitro studies and the microbiological isolation. M.A. S. performed the histopathological analysis. M.E.E. and G.I.F. performed acute toxicity experiment and determined the LD_{50}, the laboratory experiments, and sample collection. M.A.E., M.S.K., and A.H.S. performed the biochemical analysis.

Financial support and sponsorship

Nil.

Conflicts of interest

There are no conflicts of interest.

References

1 Uçmak ZG, Kurban I, Uçmak M. Evaluation of vascularization in the walls of preovulatory follicles in mares with endometritis. Theriogenology 2020; 157:79–84.

2 Cui L, Wang H, Lin J, Wang Y, Dong J, Li J, Li J. Progesterone inhibits inflammatory response in E. coli- or LPS-Stimulated bovine endometrial epithelial cells by NF-κB and MAPK pathways. Dev Compar Immunol 2020; 105:103568.

3 Miao Y, Ishfaq M, Liu Y, Wu Z, Wang J, Li R, *et al.* Baicalin attenuates endometritis in a rabbit model induced by infection with *Escherichia coli* and *Staphylococcus aureus* via NF-κB and JNK signaling pathways. Domest Anim Endocrinol 2021; 74:106508.

4 Li W, Fu K, Lv X, Wang Y, Wang J, Li H, *et al.* Lactoferrin suppresses lipopolysaccharide-induced endometritis in mice via down-regulation of the NF-κB pathway. Int Immunopharmacol 2015; 28:695–699.

5 Jiang PY, Zhu XJ, Zhang YN, Zhou FF, Yang XF. Protective effects of apigenin on LPS-induced endometritis via activating Nrf2 signaling pathway. Microb Pathog 2018; 123:139–143.

6 Zhu H, Li W, Wang Z, Chen J, Ding M, Han L. TREM-1 deficiency attenuates the inflammatory responses in LPS-induced murine endometritis. Microb Biotechnol 2019; 12:1337–1345.

7 Duchesne R, Castagnet S, Maillard K, Petry S, Cattoir V, Giard JC, Leon A. In vitro antimicrobial susceptibility of equine clinical isolates from France, 2006–2016. J Glob Antimicrob Resist 2019; 19:144–153.

8 de Lagarde M, Larrieu C, Praud K, Schouler C, Doublet B, Sallé G, *et al.* Prevalence, risk factors, and characterization of multidrug resistant and extended spectrum β-lactamase/AmpC β-lactamase producing *Escherichia coli* in healthy horses in France in 2015. J Vet Int Med 2019; 33:902–911.

9 Abou El-Nour KMM, Eftaiha A, Al-Warthan A, Ammar RAA. Synthesis and applications of silver nano-particles. Arab J Chem 2010; 3:135–140.

10 Ahmed S, Ahmad M, Swami BL, Ikram S. A review on plants extract mediated synthesis of silver nano-particles for antimicrobial applications: a green expertise. J Adv Res 2016; 7:17–28.

11 Nascimento GGF, Locatelli J, Freitas PC, Silva GL Antibacterial activity of plant extracts and phytochemicals on antibioticresistant bacteria. Braz J Microbiol 2000; 31:247–256.

12 Sharoba AM, El Mansy HA, El Tanahy HH, ElWaseif KH, Ibrahim MA. Chemical composition, antioxidant and antimicrobial properties of the essential oils and extracts of some aromatic plants. Middle East J Appl Sci 2015; 5:344–352.

13 Singh K, Panghal M, Kadyan S, Chaudhary U, Yadav JP. Green silver nano-particles of *Phyllanthus amarus*: as an antibacterial agent against multi drug resistant clinical isolates of *Pseudomonas aeruginosa*. J Nanobiotechnol 2014; 12:1–9.

14 Singh P, Kim Y-J., Zhang D, Yang D-C. Biological synthesis of nano-particles from plants and microorganisms. Trends Biotechnol 2016; 34:588–599.

15 Girón-Vázquez N, Gomez-Gutierrez C, Soto-Robles C, Nava O, Lugo-Medina E, Castrejon-Sanchez V, *et al.* Study of the effect of *Persea americana* seed in the green synthesis of silver nano-particles and their antimicrobial properties. Results Phy 2019; 13:102142.

16 Gavade N, Kadam A, Suwarnkar M, Ghodake V, Garadkar K. Biogenic synthesis of multi-applicative silver nano-particles by using *Ziziphus jujuba* leaf extract. Spectrochim Acta A Mol Biomol Spectrosc 2015; 136:953–960.

17 Onitsuka S, Hamada T, Okamura H. Preparation of antimicrobial gold and silver nano-particles from tea leaf extracts. Colloids Surf B 2019; 173:242–248.

18 Rajan A, Rajan AR, Philip D. *Elettaria cardamomum* seed mediated rapid synthesis of gold nano-particles and its biological activities. Open Nano 2017; 2:1–8.

19 Ma⊠átková O, Michailidu J, Miškovská A, Kolouchová I, Masák J, Čejková A. Antimicrobial properties and applications of metal nano-particles biosynthesized by green methods. Biotechnol Adv 2022; 58:107905.

20 Abolghasemi R, Haghighi M, Solgi M, Mobinikhaledi A. Rapid synthesis of ZnO nano-particles by waste thyme (*Thymus vulgaris L*). Int J Environ Sci Technol 2019; 16:6985–6990.

21 Aboelmaaty AM, Omara ST, Aly MS, Kotp MS, Ali AH. The antibacterial and anti-inflammatory effects of zinc oxide nano-particles synthesized by *Thymus vulgaris* medicinal plant against *Escherichia coli* and *Escherichia coli* lipopolysaccharides. Egypt Pharm J 2022; 21:1–14.

22 Riddle WT, LeBlanc MM, Stromberq AJ. Relationships between uterine culture, cytology and pregnancy rates in Thoroughbred practice. Theriogenology 2007; 68:395–402.

23 Winn W, Allen S, Janda W, Koneman E, Procop G, Schreckenberger P, Woods G. Koneman's Color Atlas and Textbook of Diagnostic Microbiology 6th ed. New York, USA: Lippincott Williams and Wilkins 2006.

24 CLSI. Performance Standards for Antimicrobial Disk Susceptibility Tests; Twenty-Fourth Informational Supplement National Committee for Clinical Laboratory Standards institute. Wayne, PA, USA: CLSI; 2014.

25 Cruickshank R, Duguid JP, Masion BP, Swain RH. Medical microbiology. 12th ed. Edinburgh, London, New York: Churchill Livingstone; 1979.

26 Hegazi AG, El-Houssiny AS, Fouad EA. Egyptian propolis potential antibacterial activity of propolis-encapsulated alginate nano-particles against different pathogenic bacteria strains. Adv Natl Sci 10.

27 Hashizume T, Komatsu T, Okumoto Y, Ogashiwa M, Kemi M, Takase Z. Therapeutic effects of imipenem-cilastatin on experimental intrauterine infections in rats. Antimicrob Agents Chemother 1987; 31:578–581.

28 Kramer BW, Moss TJ, Willet KE, Newnham JP, Sly PD, Kallapur SG, *et al.* Dose and time response after intraamniotic endotoxin in preterm lambs. Am J Respir Crit Care Med 2001; 164:982–988.

29 Suvarna KS, Layton C, Bancroft JD. Bancroft's Theory and Practice of Histological Techniques, British Library Cataloguing in Publication Data, 7th ed. China: Elsevier Health Sciences; 2018.

30 Thamer NA, AL-Mashhady LA. Acute toxicity of green synthesis of silver nano-particles using crocus sativud l on white albino rats. Int J Phytopharmacol 2016; 7:13–16.

31 Hoseini-Alfatemi SM, Fallah F, Armin S, Hafizi M, Karimi A, Kalanaky S. Evaluation of blood and liver cytotoxicity and apoptosis-necrosis induced by nanochelating based silver nano-particles in mouse model. Iran J Pharma Res 2020; 19:207–218.

32 Landsiedel R, Hahn D, Ossig R, Ritz S, Sauer L, Buesen R, *et al.* Gut microbiome and plasma metabolome changes in rats after oral gavage of nano-particles: sensitive indicators of possible adverse health effects. Part Fibre Toxicol 2022; 19:21.

33 Mao BH, Luo YK, Wang BJ, Chen CW, Cheng FY, Lee YH, *et al.* Use of an in-silico knowledge discovery approach to determine mechanistic studies of silver nano-particles-induced toxicity from in vitro to in vivo. Part Fibre Toxicol 2022; 19:6.

34 Tarbali S, Karami Mehrian S, Khezri S. Toxicity effects evaluation of green synthesized silver nano-particles on intraperitoneally exposed male Wistar rats. Toxicol Mech Methods 2022; 19:1–13.

35 Shin SH, Ye MK, Kim HS, Kang HS. The effects of nano-silver on the proliferation and cytokine expression by peripheral blood mononuclear cells. Int Immunopharmacol 2007; 7:1813–1818.

36 Yousef MI, Abuzreda AA, Kamel MA. Cardiotoxicity and lung toxicity in male rats induced by long-term exposure to iron oxide and silver nano-particles. Exp Therap Med 2019; 18:4329–4339.

37 Zubair M, Azeem M, Mumtaz R, Younas M, Adrees M, Zubair E, *et al.* Green synthesis and characterization of silver nano-particles from Acacia nilotica and their anticancer, antidiabetic and antioxidant efficacy. Environ Poll 2022; 304:119249.

38 Essghaier B, Toukabri N, Dridi R, Hannachi H, Limam I, Mottola F, *et al.* First report of the biosynthesis and characterization of silver nano-particles using scabiosa atropurpurea subsp maritima fruit extracts and their antioxidant, antimicrobial and cytotoxic properties. Nanomaterials (Basel) 2022; 12:1585.

39 Afreen A, Ahmed R, Mehboob S, Tariq M, Alghamdi HA, Zahid AA, *et al.* Phytochemical-assisted biosynthesis of silver nano-particles from Ajuga bracteosa for biomedical applications. Mat Res Exp 2020; 7:075404.

40 Elkhawass EA, Mohallal ME, Soliman MM. Acute toxicity of different sizes of silver nano-particles intraperitonally injected in balb/c mice using two toxicological methods. Int J Pharma Pharma Sci 2015; 7:94–99.

41 Wang L, Hu C, Shao L. The antimicrobial activity of nano-particles: present situation and prospects for the future. Int J Nanomed 2017; 12:1227–1249.

42 Cho YM, Mizuta Y, Akagi JI, Toyoda T, Sone M, Ogawa K. Size-dependent acute toxicity of silver nano-particles in mice. J Toxicol Pathol 2018; 31:73–80.

43 Park K. Toxicokinetic differences and toxicities of silver nano-particles and silver ions in rats after single oral administration. J Toxicol Environ Health A 2013; 76:1246–1260.

44 Sirotkin AV, Alexa R, Stochmalova A, Scsukova S. Plant isoflavones can affect accumulation and impact of silver and titania nano-particles on ovarian cells. Endocrinol Regul 2021; 55:52–60.

45 Tabandeh MR, Samie KA, Mobarakeh ES, Khadem MD, Jozaie S. Silver nano-particles induce oxidative stress, apoptosis and impaired steroidogenesis in ovarian granulosa cells of cattle. Anim Reprod Sci 2022; 236:106908.

46 Kang SJ, Ryoo IG, Lee YJ, Kwak MK. Role of the Nrf2. heme oxygenase-1 pathway in silver nanoparticle-mediated cytotoxicity. Toxicol Appl Pharmacol 2012; 258:89–98.

47 Jiang X, Wang L, Ji Y, Tang J, Tian X, Cao M. Interference of steroidogenesis by gold nanorod core/silver shell nanostructures: implications for reproductive toxicity of silver nanomaterials. Small 2017; 13:10.

48 Mirzaei M, Razi M, Sadrkhanlou R. Nanosilver particles increase follicular atresia: Correlation with oxidative stress and aromatization. Environ Toxicol 2017; 32:2244–2255.

49 Fu K, Lv X, Li W, Wang Y, Li H, Tian W. Berberine hydrochloride attenuates lipopolysaccharide-induced endometritis in mice by suppressing activation of NF-κB signal pathway. Int Immunopharmacol 2015; 24:128–132.

50 Tiwari A, Singh P, Jaitley P, Sharma S, Prakash A, Mandil R. *Eucalyptus robusta* leaves methanolic extract suppresses inflammatory mediators by specifically targeting TLR4/TLR9, MPO, COX2, iNOS and inflammatory cytokines in experimentally-induced endometritis in rats. J Ethnopharmacol 2018; 213:149–158.

51 Liang Y, Shen T, Ming Q, Han G, Zhang Y, Liang J, *et al.* Alpinetin ameliorates inflammatory response in LPS-induced endometritis in mice. Int Immunopharmacol 2018; 62:309–312.

52 Ferdous Z, Nemmar A. Health impact of silver nano-particles: a review of the biodistribution and toxicity following various routes of exposure. Int J Mol Sci 2020; 21:2375.

53 Stebounova LV, Adamcakova-Dodd A, Kim JS, Park H, O'Shaughnessy PT, Grassian VH, *et al.* Nanosilver induces minimal lung toxicity or inflammation in a subacute murine inhalation model. Part Fibre Toxicol 2011; 8:5.

54 Ajdary M, Eghbali S, Mahabadi VP, Keyhanfar F, Varma RS. Toxicity of silver nano-particles on endometrial receptivity in female mice. Can J Physiol Pharmacol 2021; 99:1264–1271.

55 Song KS, Sung JH, Ji JH, Lee JH, Lee JS, Ryu HR, *et al.* Recovery from silver-nanoparticle-exposure-induced lung inflammation and lung function changes in Sprague Dawley rats. Nanotoxicology 2013; 7:169–180.

56 Sung JH, Ji JH, Park JD, Yoon JU, Kim DS, Jeon KS, *et al.* Subchronic inhalation toxicity of silver nano-particles. Toxicol Sci 2008; 108:452–461.

57 Kim W-Y., Kim J, Park JD, Ryu HY, Yu IJ. Histological study of gender differences in accumulation of silver nano-particles in kidneys of Fischer 344 rats. J Toxicol Environ Health A 2009; 72:1279–1284.

58 Jiang X, Hu Y, Zhou Y, Chen J, Sun C, Chen Z, *et al.* Irisin protects female mice with LPS-induced endometritis through the AMPK/NF-κB pathway. Iran J Basic Med Sci 2021; 24:1247–1253.

59 Han S, Cicek AF, Tokmak A, Yildirir Ustun T, Ercan Gokay N, Uludag MO, *et al.* Effects of resveratrol on receptor expression and serum levels of estrogen and progesterone in the rat endometritis model. Reprod Sci 2021; 28:2610–2622.

60 Wu H, Jiang K, Yin N, Ma X, Zhao G, Qiu C, *et al.* Thymol mitigates lipopolysaccharide-induced endometritis by regulating the T LR4. and ROS-mediated NF-κB signaling pathways. Oncotarget 2017; 8:20042–20055.

61 Piersanti RL, Zimpel R, Molinari PCC, Dickson MJ, Ma Z, Jeong KC, *et al.* A model of clinical endometritis in Holstein heifers using pathogenic *Escherichia coli* and *Trueperella pyogenes*. J Dairy Sci 2019; 102:2686–2697.

62 Jana B, Kucharski J, Ziecik AJ. Effect of intrauterine infusion of *Escherichia coli* on hormonal patterns in gilts during the oestrous cycle. Reprod Nutr Dev 2004; 44:37–48.

63 Lüttgenau J, Lingemann B, Wellnitz O, Hankele AK, Schmicke M, Ulbrich SE, *et al.* Repeated intrauterine infusions of lipopolysaccharide alter gene expression and lifespan of the bovine corpus luteum. J Dairy Sci 2016; 99:6639–6653.

64 Herath S, Williams EJ, Lilly ST, Gilbert RO, Dobson H, Bryant CE, *et al.* Ovarian follicular cells have innate immune capabilities that modulate their endocrine function. Reproduction 2007; 134:683–693.

65 Dickson MJ, Piersanti RL, Ramirez-Hernandez R, de Oliveira EB, Bishop JV, Hansen TR, *et al.* Experimentally induced endometritis impairs the developmental capacity of bovine oocytes. Biol Reprod 2020; 103:508–520.

66 Li T, Yang N, Teng D, Mao R, Hao Y, Wang X, *et al.* C-terminal mini-PEGylation of a marine peptide N6 had potent antibacterial and anti-inflammatory properties against *Escherichia coli* and Salmonella strains in vitro and in vivo. BMC Microbiol 2022; 22:128.

67 Lowes DA, Webster NR, Murphy MP, Galley HF. Antioxidants that protect mitochondria reduce interleukin-6 and oxidative stress, improve mitochondrial function, and reduce biochemical markers of organ dysfunction in a rat model of acute sepsis. Br J Anesth 2013; 110:472–480.